Modeling NAPL dissolution and biodegradation interactions: effect of toxicity and biomass growth limitations

C. Gallo[a b] and S.M. Hassanizadeh[a]

[a]Dept. of Civil Engineering and Geosciences, TUDelft, The Netherlands

[b]CRS4, VI Strada Ovest, Z.I. Macchiareddu, UTA (CA), Italy

This work focuses on some aspects of the interactions between NAPL dissolution, molecular diffusion and biodegradation processes. Starting from a test problem based on a real field scenario, a one-dimensional model is set up. A number of simulations are run using different biomass distributions, varying diffusion coefficients and biological kinetic rates. Results indicate that under ideal conditions biomass distribution along the column does not make a real difference in terms of total amount of dissolved oil degraded. Results change dramatically when introducing limitations in the growth of biomass and the effects of toxicity into the model. Both of these are modelled as functions for which some threshold or bounding levels are specified. In particular, toxicity function is derived from some phenomenogical considerations, since, at least to the author's knowledge, no documentation in the literature is available in this regard. Constrained biomass growth and contaminant toxicity have been found to yield results consistent with field data on contaminant distribution. This would support our presumption that biomass growth constraint and toxicity play a major role in reducing natural attenuation efficiency.

1. INTRODUCTION

In this work, we have studied the combination of biodegradation and dissolution. There are a number of studies on NAPL dissolution mechanisms and properties of two-phase flow ([5,7,4,6]). Similarly, much work has been carried out on biodegradation of dissolved contaminants and different mathematical/numerical approaches have been presented in the literature (see [2] and references listed therein). However, there are only a few studies that have dealt with the coupling between the two processes. This situation typically occurs in *near-to-source* contamination scenarios in which both NAPL phase and active biomass are present. Near-to-source does not imply a precise measure in terms of distance from the spill location. However, it should be intended as "sufficiently close" to the contaminant spill so that the concurrence of processes such as NAPL dissolution, transport of dissolved oil in the aqueous phase, biodegradation, biomass growth, and toxicity effects should be accounted for. The relative weight of each process may play a role on the overall degradation.

This work is a continuation of the research presented in our previous paper [3]. The current focus is on the effect of molecular diffusion and biomass distribution on NAPL dissolution and biodegradation. This is discussed in light of the presence of "nonidealities" in the system. The word "nonidealities" stands for those processes which may diminish, inhibit, or definitetely stop the biodegradation process. Two degradation-limiting processes are considered, that is, biomass growth limitations and toxicity of the contaminant for bacterial population. These factors may have a strong impact on contaminant biodegradation, but, to our knowledge, no extensive study has been presented in order to quantify these effects. In this paper, preliminary results are presented on the topics.

2. GOVERNING EQUATIONS

NAPL dissolution, dissolved-oil transport and biodegradation are processes that are included in the model. Dissolved-oil diffusive transport in the aqueous phase is modeled as follows:

$$\phi S_l \frac{\partial C^S}{\partial t} + D \frac{\partial^2 C^S}{\partial x^2} = E_{ln} - \phi S_l B^S. \tag{1}$$

where C^S is concentration of dissolved NAPL, t is time, ϕ is porosity, S_l is aqueous phase saturation, v_l is aqueous phase velocity and D is molecular diffusion coefficient. The term E_{ln} is linearly proportional to the difference between the solubility limit of NAPL, C^S_{eq}, and its actual concentration, C^S, i.e.

$$E_{ln} = \phi S_n k_{do} \left(C^S_{eq} - C^S \right). \tag{2}$$

k_{do} is the dissolution rate coefficient and S_n is NAPL saturation. The term B^S designates the biodegradation rate and takes the form

$$B^S = C^X Y \mu_0 \left[\frac{C^S}{K_{1/2} + C^S} \right], \tag{3}$$

where μ_0 is the maximum degradation rate, $K_{1/2}$ is the half-saturation constant, C^X is biomass concentration, and Y is a yield coefficient.

Finally, the rate of microbial growth/decay reads as follows:

$$\frac{1}{C^X} \frac{\partial C^X}{\partial t} = \mu_0 \left(\frac{C^S}{K_{1/2} + C^S} \right) \cdot \mathcal{F} - k_d. \tag{4}$$

k_d is the decay rate coefficient, while $\mathcal{F}$ incorporates nonidealities in the system. $\mathcal{F} = 1$ unless explicitly specified (see below).

3. SIMULATION RESULTS AND DISCUSSION

3.1. Testcase description

The test problem studied here is based on the fractured field site at Ringe, Denmark. We consider a porous medium in which two zones can be identified: fractures/high-permeability and matrix/low-permeability zones. Flow of fluids is assumed to occur within the fractures only. Thus, the bulk fluid flow within the matrix is assumed negligible and the migration of the contaminant in the soil matrix is only due to diffusion. Biodegradation is assumed to occur in the soil matrix only. Fractures/high permeability soil may contain free NAPL and this may prohibit biomass growth due to toxicity effects. Moreover, the volume fraction of high-permeability soil is generally smaller than the fraction of low-permeability soil matrix and, thus, its contribution to the biodegradation process is negligible. So, we focus our simulations on the diffusion into and dissolution and biodegradation within the matrix. We simulate the matrix zone as a 1-D column of 10 cm long. filled with a porous medium. The column is discretized into 50 elements of 0.002 m long. The column is assumed to be fully saturated with water except for the first one centimeter (next to the fracture) where we have a residual NAPL saturation of 0.20. ($S_n = 0.2$, $S_l = 0.8$ for $0 \leq x < 1$ cm, $S_l = 1$ elsewhere). The total simulation time is 40 days and a time step of 34 s (0.0004 days). Initial contaminant concentration is assumed to be zero. The initial biomass concentration is 3.53 x $10^{-}3$ kg/m^3. Starting with this initial condition, the column is assumed to be sealed. Zero-diffusion boundary condition is set for the transport. Under these conditions, NAPL dissolution, dissolved-NAPL diffusion and biodegradation are the only processes taking place in the system. Other data used in the simulation are reported in table 1.

Table 1
Biological parameters.

Parameter	value	parameter	value
K^S (kg/m^3)	0.120	Y^S (-)	3.56
k_d (1/s)	2.3E-07	μ_0 (1/s)	5.E-05
$C^{S,eq}$ (kg/m^3)	5.E-03	k_{do} (m^2/s)	6.9E-11

3.2. Effect of Diffusion

The first set of simulations were run considering diffusion varying within two orders of magnitude, that is, $D = [1.4{*}10^{-10}, 1.4{*}10^{-8}]$ m^2/s. As simulation starts, NAPL dissolves and invades the column at a rate that is a function of the diffusion coefficient: the higher the diffusion, the higher the concentration within the column. Figure 1 (left) shows the mass present in the column as a function of time for different values of the diffusion coefficient. The dissolved-NAPL mass present in the column increases proportionally to diffusion coefficient, but for the largest D the curve shows a knee. This corresponds to the moment that $C^S = C^S_{eq}$ and that the column is saturated with dissolved NAPL. The dissolved-oil mass present in the column is lower when biodegradation is active, but the total dissolved NAPL equals the sum of the actual mass present in the column and the mass degraded by bacteria. Thus, as shown in Figure 1-right, the total mass of dissolved NAPL (i.e. the organic substrate inflow) is much higher than in the previous case. This indicates that biodegradation can really enhance free-phase dissolution, both in terms of rate of dissolution and in terms of amount of mass dissolved.

3.3. Biomass distribution effects

Initial biomass distribution can be important when dealing with fractured soils. As reported in [1], active biomass is located in a small region of soil adjacent to fractures. In many cases, only the fraction of the soil matrix containing larger pores, which are expected

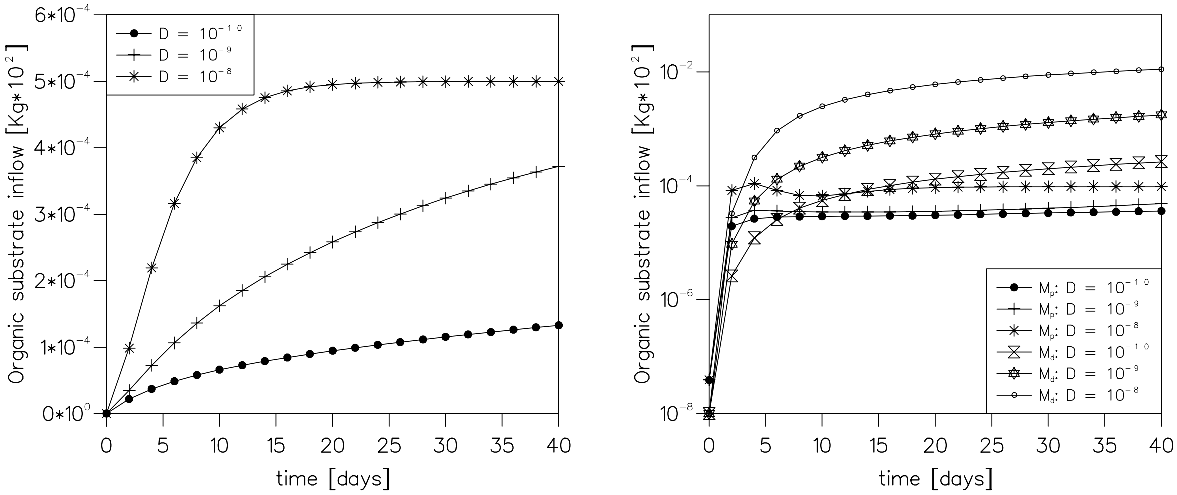

Figure 1. NAPL dissolved in the column without biodegradation (left) and with biodegradation (right) (M_p: mass present in the aqueous phase; M_d: mass degraded).

to be located close to fractures and/or zones of high permeability, are able to host bacterial growth. The rest of the soil is inert with respect to biodegration. Two initial biomass distributions are considered: BioF (full; that is, $C^X(t = 0) = 0.0$ for $0 \leq x < 1$ cm, $C^X(t = 0) = 0.0353$ kg/m^3 otherwise); BioP (partial; that is, $C^X(t = 0) = 0.0$ for $0 \leq x < 1$ cm, $C^X(t = 0) = 0.0353$ kg/m^3, for $1 \leq x < 2$ cm, $C^X(t = 0) = 0.0$ otherwise). Simulations similar to those described in the previous section (for varying D) are now carried out here with two different spatial biomass distributions BioP and BioF. Results indicated that concentration distribution of dissolved oil in the BioF and BioP cases are almost identical. This can be explained when examining biomass distribution at the end of the simulation. C^X profiles for different values of the diffusion coefficient and various biodegradation kinetics are almost identical, except for low μ_0 in which some differences are present at early times. Plots of biomass concentration vs space and time are shown in Figure 2. It is apparent that for long simulation times, concentrations of dissolved oil for both cases approach pseudo steady-state conditions are reached.

4. INTRODUCING NON-IDEALITIES IN THE SYSTEM

Too often non-idealities are neglected in simulations of biodegradation processes. In real field applications, many factors may play a role in the degradation process and some of them are critical for increasing or decreasing the degradation rate. For example, neglecting biomass growth limitations implies that as long as dissolved oil is available, biomass can grow on and on, regardless of the volume available for accommodating biomass. This is a strong simplification and may lead to excessively optimistic predictions. Also, high concentration of dissolved contaminants may be toxic to bacteria and can inhibit either temporarily or definitely the biodegradation process. In the following paragraphs, these two factors are studied and discussed.

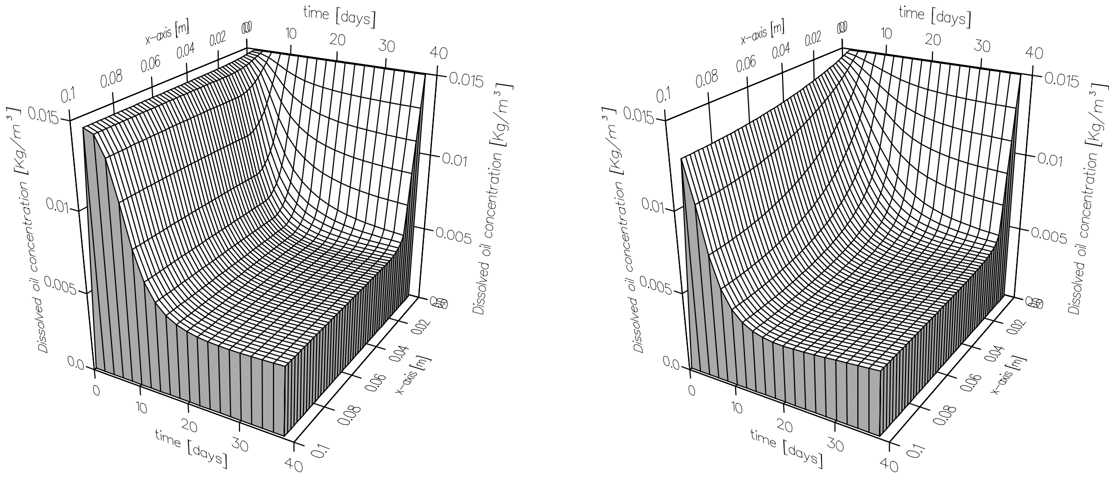

Figure 2. Biomass concentration profiles at $t = 400$ days and $\mu_0 = 1.e{-}5$ 1/s for case BioP (left) and BioF (right).

4.1. The effect of biomass growth limitations

From the mathematical point of view, biomass growth limitation can be introduced defining $\mathcal{F} = \mathcal{F}_{bgc} = (1 - C^X/C^X_{max})$ in equation (4). When $C^X \to C^X_{max}$, bacterial growth rate reduces to zero and only biomass decay ($k_d C^X$ in equation 4) may occur. In the simulations reported here, C^X_{max} is set to 10^{-1} kg/m^3. For low values of D, dissolved-oil concentration is low in the column except close to the fracture zone where NAPL is trapped. Dissolved-oil migration is also slow and biomass can degrade the incoming contaminant rate in both BioP and BioF cases. However, for large D, NAPL dissolution rate increases also and bacteria are provided with a large amount of oil to degrade per unit time. With biomass growth limited, large peaks of biomass concentration are suppressed and BioP and BioF biomass initial distributions yield different results. As shown in Figure 3, an accumulation of dissolved oil occurs in the column. In this case, biomass is able to degrade almost all dissolved oil for BioF distribution, while the same cannot be said in the BioP case whose degradation capacity is limited.

4.2. The effect of contaminant toxicity

In many cases, a contaminant that is normaly degraded at low concentration, may become toxic for bacteria at high concentration. This has an impact on the effectiveness of overal degradation process. Consider trapped NAPL that dissolves and diffuses along the column. If any active biomass is present, biodegradation begins. Depending on the relative weights of dissolution rate and molecular diffusion coefficient, if diffusion process is not sufficiently fast, dissolved oil may accumulate. Thus, if C^S approaches the toxicity level, indicated with C^S_{tox}, biodegradation rate decreases and the biomass become inactive for $C^S \geq C^S_{tox}$. Based on this reasoning, we propose to model the toxicity effect by setting $\mathcal{F} = \mathcal{F}_{tox} = 1 - (C^S/C^S_{tox})^2$ for $C^S \leq C^S_{tox}$, and $\mathcal{F}_{tox} = 0$ for $C^S > C^S_{tox}$. If C^S falls below C^S_{tox}, biodegradation resumes and biomass can continue to grow. For the simulations

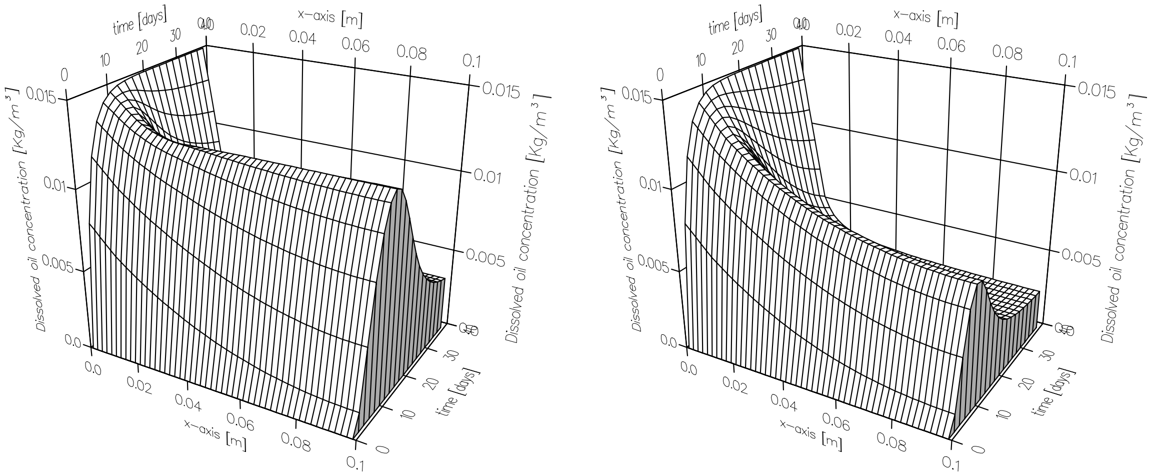

Figure 3. Dissolved-oil concentration profile in time and space with μ_0 =2.5E-5 1/s for cases BioP (left) and BioF (right) with biomass growth limitation.

reported here, C^S_{tox} is set to 5x10^{-3} kg/m^3 and D = 1.4x10^{-9} m^2/s. Simulation results obtained for a wide range of values of k_{do} and μ_0, are shown in Figure 4-left. These results indicate that there is a critical value of the maximum degradation constant μ_0 below which biodegradation decreases sharply. This critical value depends on the value of the mass dissolution rate coefficient, k_{do}, and diffusion coefficient, D. This result does not give any real insight in terms of practical applications, given the artificial and sharp transition between the two zones which seems mainly a mathematical outcome. It would be probably possible to find a functional relationship between k_{do}, D, and μ_0 for estimating *a-priori* the critical range of conditions for biodegradation to occur successfully. However, it is not in the purpose of this work to come up with a mathematical correlation of this dependency. We believe that this correlation would be strongly test-case dependent.

4.3. Combination of biomass-growth constraint and toxicity effects

The combination of the two nonidealities introduced here, can be included in equation (4) by defining $\mathcal{F} = \mathcal{F}_{bgc} \cdot \mathcal{F}_{tox}$. The numerical investigation is conducted considering a column of 100 cm and simulation time of 400 days. In the simulations, variations of the three most important parameters of the model, that is, NAPL dissolution rate constant k_{do}, molecular diffusion coefficient D, and the degradation kinetic rate constant μ_0 have been considered. Figure 4-right is an example of how the total dissolved-oil mass is influenced by the degradation rate and the dissolution rate coefficient. Other parameters such as molecular diffusion and yield coefficient are, of course, also important. These effects must be studied separately in a systematic manner.

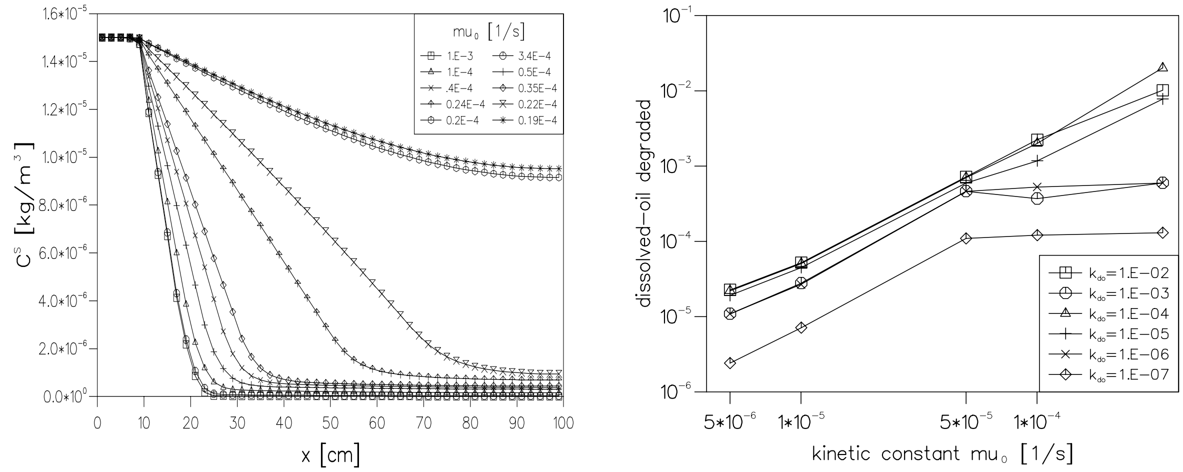

Figure 4. C^S profiles as a function of μ_0 (left - only toxicity active). Dissolved-oil degraded as a function of μ_0 and k_{do} (right).

5. CONCLUSIONS

Several processes occurring in a NAPL dissolution scenario and their impact on natural biodegradation have been investigated. Preliminary results indicated that when nonidealities, such as biomass growth limitation and toxicity, are neglected, spatial biomass distribution is not really critical for the overall contaminant degradation, and molecular diffusion simply dominates the equilibrium between NAPL dissolution and biodegradation. Different results are obtained when nonidealities are included in the simulations. For example, we found that initial biomass distribution is critical under biomass growth limitations. When toxicity is included, biodegradation seems to be controlled by a critical value of the maximum biodegradation rate below which biodegradation slows down significantly. More pronounced effects are obtained when biomass growth limitation and toxicity are both included. Simulation results show that toxicity plays an important role in determining the success or failure of biodegration.
Aknowledgments This research has been partly carried out in the framework of the TRIAS project "Multiphase flow and enhanced biodegradation of non-aqueous phase liquids" (Delft Cluster Project 5.1.6). The work of C. Gallo was partly supported by Sardinian Regional Authorities and by the Italian Ministry of the University (project ISR8-C11/B).

REFERENCES

1. Rosenbom A., Aamand J., Friis K., Lindgren H., and Springer N. Laboratory set-ups and experimental results. in Pore-to-Core scale-up studies of the transport properties of organic pollutants with natural attenuation. Technical Report report no. 1998/104.,

Geological survey of Denmark and Greenland, 1998.
2. P. C. de Blanc. Modeling subsurface biodegradation of non-aqueous phase liquids: a literature review. Technical Report CRWR 257, Center for Research in Water Resources, The University of Texas at Austin, J.J. Pickle Research Campus - Austin, Texas 78712, 1995.
3. C. Gallo and S. M. Hassanizadeh. Influence of biodegradation on NAPL flow and dissolution in groundwater. In L. R. Bentley et al., editor, *Proc. of the XII International Conference on Computational Methods in Water Resources*, volume I, pages 129–136, Rotterdam, Holland, 2000. A.A. Balkema.
4. P. T. Imhoff and P. R. Jaffè. An experimental study of complete dissolution of a nonaqueous phase liquid in saturated porous media. *Water Resources Research*, 29(2):307–320, 1993.
5. D. Mackay, W. Y. Shiu, A. Maijanen, and S. Feenstra. Dissolution of nonaqueous phase liquids in groundwater. *J. Contam. Hydrology*, 8:23–42, 1991.
6. S. E. Powers, L. M. Abriola, and Jr. W. J. Weber. An experimental investigation of nonaqueous phase liquid dissolution in saturated subsurface systems: Transient mass transfer rates. *Water Resources Research*, 30(2):321–332, 1994.
7. S. E. Powers, C. O. Louriero, L. M. Abriola, and Jr. Walter J. Weber. Theoretical study of the significance of nonequilibrium dissolution of nonaqueous phase liquids in subsurface systems. *Water Resour. Res.*, 27(4):463–477, 1991.